

Condensation character of a stratified flow inside a horizontal tube

Shengqiang Shen*, Rui Liu, Yong Yang, Xiaohua Liu, Juexian Chen

Key Laboratory of Liaoning Province for Desalination, School of Energy and Power Engineering, Dalian University of Technology, Dalian 116024, China

Tel. +86 (411) 84708464; Fax +86 (411) 84707963; email: zzbshen@dlut.edu.cn

Received 31 November 2010; Accepted in revised form 11 May 2011

ABSTRACT

A series of experiments was performed to investigate the steam condensation phenomenon of stratified flow inside horizontal tube in vacuum condition. Using segmented cooling mode to maintain a near-constant temperature of cooling water. Based on the experimental results, this paper analyses the influence of temperature difference and the inlet velocity of vapor on both heat flux density ratio and heat transfer coefficient ratio between water side and vapor side. It is found that inlet velocity and condensate quantity has obvious effect on both heat flux density ratio and heat transfer coefficient ratio.

Keywords: Heat flux density ratio; Heat transfer coefficient ratio; Stratified flow; Condensation; Desalination

1. Introduction

The multiple-effect distillation (MED) process is one of the main desalination method nowadays [1]. In the past for technology reason, the capacity of MED plants is lower than that of the multiple-stage flash (MSF). But as MED is more efficient thermodynamically than MSF [2], MED desalination technology causes more and more attention in recent years. Since its higher heat transfer coefficient, the horizontal tube falling film evaporator is widely used in the MED plants [3].

In a MED plant with the horizontal tube falling film evaporators, the brine gets evaporated on the outside surface of horizontal tubes and the vapor gets condensed in horizontal tubes. In the condensing process, due to the effect of gravity, the condensate collects at the bottom of the tube and its film thickness around the tube is not uniform. This non-uniformity made the condensation

inside the horizontal tube more complex than that in a vertical tube. The stratified flow of condensate collecting at the bottom of the tube will reduce the local heat transfer coefficient. The condensate thickness gathered at the bottom of the tube is related with the heat flux density and the tube length. It is clear that the understanding of the heat transfer coefficient distribution around the tube is critical for the optimum design of evaporators in a MED desalination plant.

For stratified flow in a tube, the condensate can be divided into two parts: a thick condensate layer flows at the bottom of the tube and a thin liquid film forms on the upper portion of the tube surface. Jaster and Kosky [4] firstly suggested using classical Nusselt [5] theory to analyze the heat transfer through the thin film, and the heat transfer at the bottom of the tube should be neglected. Cavallini [6], Dobson and Chato [7] considered that heat transfer that occurs in the liquid pool at the bottom of the tube might not be negligible at high mass velocity. Wang [8] found that the effect of gravity is obviously in

* Corresponding author.

the horizontal tube with large diameter, the stratified flow occurs in the whole condensation process and wall temperature distribution on the pipe circumference significantly different, and this difference increases with the tube diameter. Thome [9] considered that the simplified flow structure assumed for evaporation inside horizontal tubes by Kattanetal [10] can also be applied to condensation, where the only difference is that the top of the tube in a stratified flow will be wetted by condensation film rather than remain dry during evaporation. Peng et al. [11] analyzed the effect of the steam velocity in the film by numerical simulation, and found that, with the inlet steam velocity increasing, the shear stress in the liquid film will become greater, the film will become thinner and the heat transfer coefficient will rise. Laohalertdecha [12] studied the condensation of R134a in the tube and found that heat transfer coefficients increased with vapor quality and mass velocity.

Flow pattern maps are used to determine flow patterns by depicting flow regime transition boundaries. The well-known flow pattern maps for horizontal tubes are those of Baker [13], Mandhane et al. [14], Thome [15], Taitel and Dukler [16], Soliman [17], and Mederic et al. [18]. All of those show that when mass flow rate of the condensate is low, the flow pattern would transfer from the stratified-wavy flow into stratified flow as the vapor velocity comes down. So only stratified-wavy flow and steady stratified flow exist in the horizontal tubes of MED.

Although heat transfer coefficient of the liquid pool at the bottom of the tube is small, the wall temperature at the bottom of the tube is normally lower than the upper portion of the tube. It will have a larger temperature difference with vapor in the tube, therefore, the heat transfer occurs in the liquid pool might not be considered. This paper analyses the influence of temperature difference and the inlet velocity of vapor on heat transfer at the bottom of the tube based on experimental results. Through the experimental study on condensation character of stratified flow inside horizontal tube, this article provides technical support for structure design of evaporator in MED power plant.

2. Experimental system

The experimental system for condensation heat transfer in a horizontal tube is shown in Fig. 1. This system consists of the steam generator, the test section, vapor–liquid separator, condenser, liquid collection tank, vacuum pump, cooling water tank, pumps and other components. It could be classified as 3 subsystems as shown below. To simulate the operation condition of the multi-effect evaporation desalination system, the heat transfer coefficient and the pressure drop of the steam were measured under the saturation temperature from 40°C to 70°C [19]. Although the inlet velocity of the steam is high, the specific volume of the steam is large in the

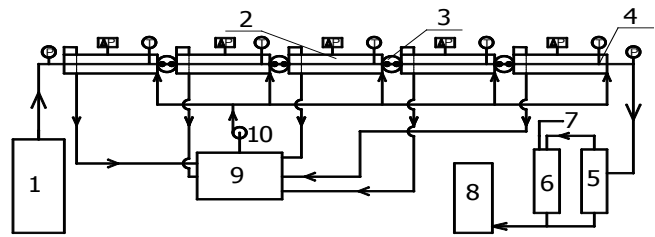


Fig. 1. Diagram of the experimental system. 1 – evaporator, 2 – test section, 3 – glass tube, 4 – temperature measuring cross section, 5 – vapor–liquid separator, 6 – condenser, 7 – vacuum pump, 8 – liquid collection tank, 9 – cooling water tank, 10 – pumps.

vacuum condition, the mass flow rate is low and decreases sharply along the tube since the condensation.

2.1. Steam subsystem

The steam subsystem is composed of five parts: the steam generator, the test section, the vapor–liquid separator, the condenser and the liquid collection tank, as shown in Fig. 1. The test section is composed of five tube-in-tube heat exchangers with each tube length of 2 m. The test tubes are made of aluminum brass, and its inner diameter is 24 mm with the tube wall thickness of 0.7 mm.

The saturation steam is produced in the evaporator by electric heating. The evaporator is connected with the test section under the same vacuum condition. In the test section the saturation steam will get condensed inside the tube and exchange heat with the cooling water outside the tube. After the test section, the steam and the condensate flow into vapor–liquid separator, and the condensate water will remain in the separator while the steam will flow to the condenser and get condensed. Both the vapor–liquid separator and the condenser have a liquid meter to measure the condensing rates. The error range of mass flow rate is less than 2%.

2.2. Cooling subsystem

The cooling subsystem is composed by cooling water tank and pumps, as shown in Fig. 1. Cooling water in cooling water tank has been heated to a certain temperature, and then is pumped to the annular cooling channel. This keeps each tube-in-tube heat exchangers having the same inlet temperature of cooling water. The flow rate of cooling water for each exchanger is the same and is calibrated. By measuring the temperature rise and flow rate of the cooling water, we might know the heat transfer rate of each tube-in-tube heat exchanger.

2.3. The instrument subsystem

Five cross sections are selected for the temperature

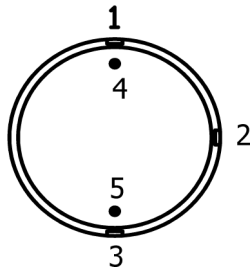


Fig. 2. Thermocouples distribution at cross section.

measurements. On each cross section five thermocouples are set respectively for measuring temperatures of the vapor and the condensate as well as the wall temperatures at the top, the middle and the bottom in the tube, as shown in Fig. 2. All the thermocouples have an accuracy of 0.1°C .

Pressure sensors are set at both the inlet and the outlet of test section to measure the steam pressure. The pressure sensor has an accuracy of ± 60 Pa. The tube side pressure drop of each exchanger is also measured by a differential manometer. It has an accuracy of ± 1 Pa.

Through the glass tube between exchangers the flow pattern could be observed. In all the experiment processes, we found only stratified flow and stratified-wavy flow pattern, as shown in Fig. 3. Those flow patterns coincide with the flow pattern maps made by the scholars mentioned above.

3. Calculation method

Ignoring the heat loss, the local average condensation heat transfer coefficient α_{in} can be expressed as:

$$Q_0 = \alpha_{in} F \Delta t, \quad \Delta t = t_s - t_w \quad (1)$$

where Q_0 is the heat transfer of one tube-in-tube heat exchanger, F is the heat transfer area of one tube-in-tube heat exchanger, Δt is the temperature difference, t_s is the saturation temperature of vapor, and t_w is the temperature of tube wall.

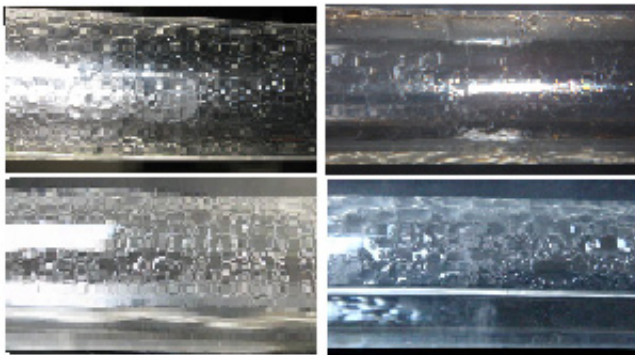


Fig. 3. Flow patterns inside the glass tube.

As the tube wall is very thin, the heat conduction in the wall along the axial and circumferential directions can be ignored.

Each tube-in-tube exchanger has the same inlet temperature and mass flow rate of cooling water, and the cooling water inlet is near the measuring cross section. Assuming that the heat transfer coefficient at the cooling water side of each exchanger is equal, then the heat flux densities on the top and at bottom of the tube can be calculated respectively by Eq. (2).

$$q_i = \alpha_{out} (t_{wi} - t_i), \quad i = s, c \quad (2)$$

where q_i is heat flux density, α_{out} is the heat transfer coefficient at the cooling water side which is assumed to be constant, t_i is the average temperature of the cooling water, t_{ws} refers to the wall temperature at the upper portion of the tube on the vapor side and t_{wc} is the wall temperature at the bottom of the tube on the condensate side.

To study the stratification effect on the heat transfer in tube, two dimensionless parameters are defined: the heat flux density ratio (C) between the condensate side and the vapor side, and the heat transfer coefficient ratio (B) between the condensate side and the vapor side. They are expressed as:

$$C = \frac{q_c}{q_s} = \frac{(t_{wc} - t_l)}{t_{ws} - t_l} \quad (3)$$

$$B = \frac{\alpha_c}{\alpha_s} = \frac{q_c / \Delta t_c}{q_s / \Delta t_s} = \frac{q_n / (t_s - t_{wc})}{q_s / (t_s - t_{ws})} \quad (4)$$

The vapor quality x is the ratio between the local mass flow of vapor and the total mass flow at the entrance of the tube. It can be expressed as

$$x = 1 - \frac{Q_c}{m\gamma} \quad (5)$$

where Q_c is the total heat transfer from the entrance of test section to the local test point, m is the mass flow at the entrance, γ is the latent heat of vaporization at saturated temperature.

4. Experimental results and analysis

4.1. Temperature distribution in the circumferential direction

Fig. 4 presents the wall temperature distribution along the tube axis at the inlet saturation temperature of 56.6°C and inlet steam velocity of 56 m/s. The wall temperatures at the top and middle of the tube are nearly the same, but the temperature at the bottom is lower than that at other positions. This indicates that the condensate exists along the tube and affects the temperature distribution. The wall temperature decreases with the length. The reason might be that under the influence of the flow resistance,

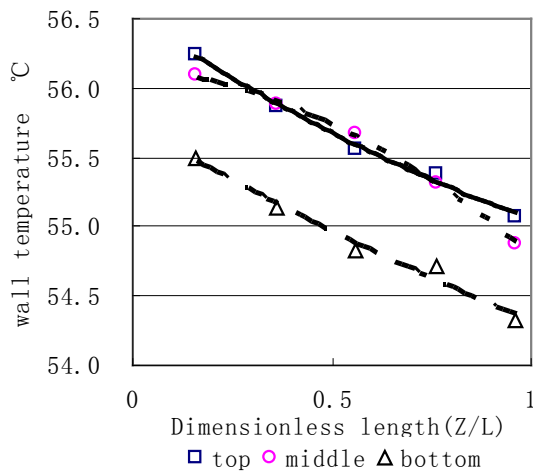


Fig. 4. Wall temperature distribution at the circumferential direction along the tube axis.

the saturation temperature of steam reduces while the wall temperature decreases with the steam saturation temperature. Even though the lowering down of the temperature is only a little more than 1°C, its influence on heat transfer is remarkable since the temperature difference in a MED desalination plant is only 2–3°C.

4.2. Impact of temperature difference on condensation heat transfer

Fig. 5 and Fig. 6 are heat flux density ratio and heat transfer coefficient at the condition of inlet saturation temperature 56.6°C, inlet velocity 56 m/s and temperature difference between cooling and steam being 4°C, 6°C and 8°C, respectively.

Fig. 5 shows the heat flux density ratio at different temperature differences. The results show that the temperature difference has little effect on the heat flux density ratio, but the vapor quality has an apparent impact on it. In the front part of the tube, the heat transfer rate at the bottom is higher than 75% of that on the top. With the decrease of the vapor quality, the depth of the condensate gets increased and the portion of heat transfer through condensate is lowering down. With the decrease of the vapor quality, the flow pattern transfers either from wavy stratified to steady stratified. The condensation heat transfer coefficient at bottom of the tube is around 3/4 of that on the top of the tube. This shows that the heat transfer through condensate should not be neglected.

The heat transfer coefficient at the bottom of the tube in different temperature differences shown in Fig. 6. The same as the heat flux density ratio, the heat transfer coefficient at the bottom of tube increases with the vapor quality, and it has little relationship with the temperature difference.

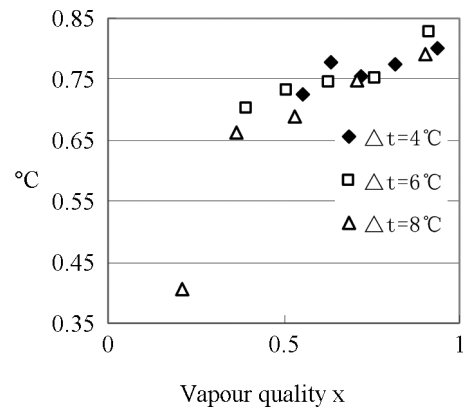


Fig. 5. Heat flux density ratio at different temperature differences.

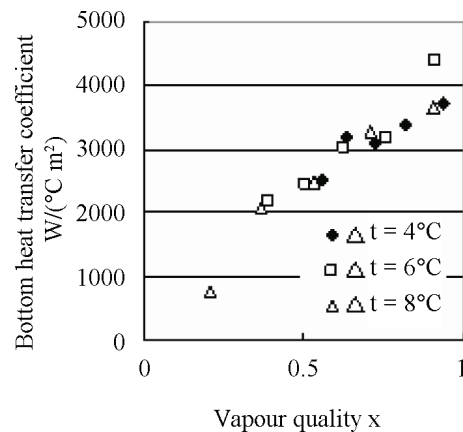


Fig. 6. Heat transfer coefficient at the bottom of tube at different temperature differences.

4.3. Impact of steam mass flow rate on the condensation heat transfer

Figs. 7–10 are experimental results at a inlet saturation temperature of 56.5°C with temperature difference of 4°C for inlet velocity of steam from 56 m/s to 27 m/s.

Fig. 7 shows the heat flux density ratio at different inlet velocity. The heat flux density ratio increases with the mass flow rate at the same dimensionless length. As the velocity of the condensation film is controlled by the shear stress between condensate and steam, the velocity of condensation film will increased with the steam velocity. The velocity of condensation enhances the heat transfer coefficient in two ways. Firstly, it increases the disturbance of the condensate. Secondly, it reduces the condensate thickness which results in the decreasing of the thermal resistance. But when the velocity of steam is higher than a certain value, such as 47 m/s and 56 m/s in Fig. 3, its effect on the enhancement of heat transfer coefficient is not obvious.

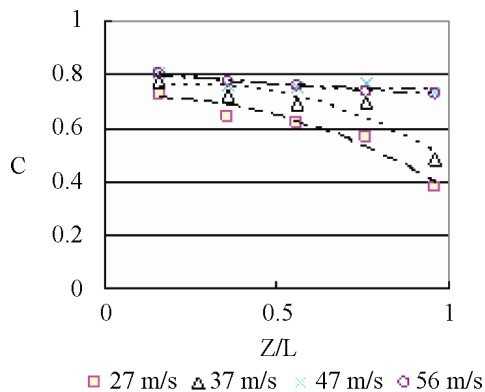


Fig. 7. Heat flux density ratio at different inlet velocities.

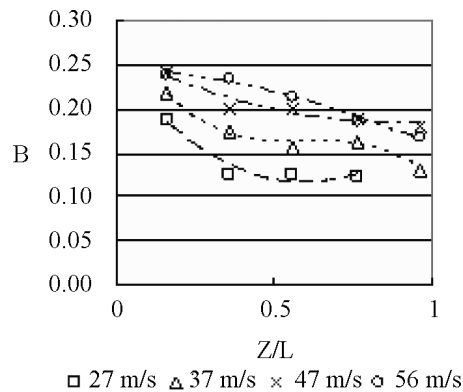


Fig. 8. Heat transfer coefficient ratio at different inlet velocities.

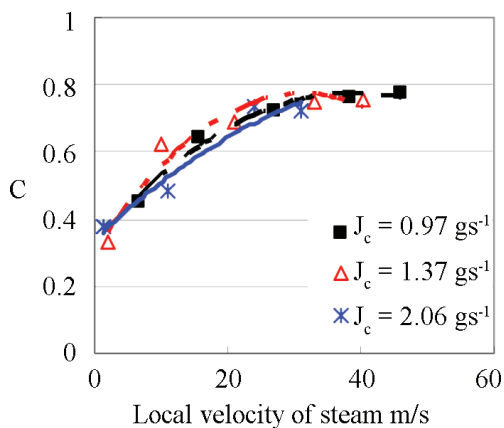


Fig. 9. Heat flux density ratio with the local steam velocity.

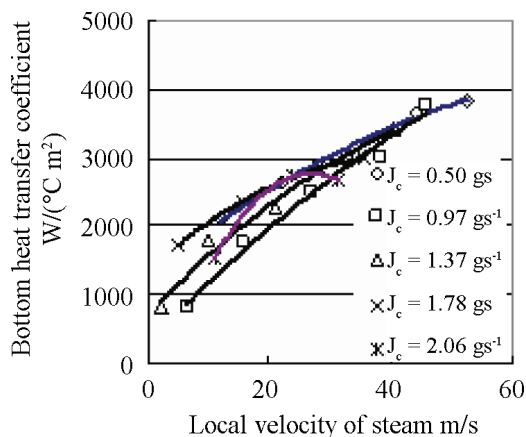


Fig. 10. Bottom heat transfer coefficient with the local steam velocity.

Fig. 8 shows the heat transfer coefficient ratio at different inlet velocity. Comparing with the figure 4, although the heat transfer coefficient is relatively low (lower than a quarter of the vapor side), the heat flux density ratio is not negligible, because the temperature difference at the bottom of tube is larger than that on the upper portion.

The curves of heat flux density ratio with the local steam velocity are shown in Fig. 9 and the heat transfer coefficient at the bottom of the tube is shown in Fig. 10. The heat flux density ratio and heat transfer coefficient at the bottom of tube is mainly affected by the local vapor velocity, they all decrease with the local vapor velocity decreasing. But the heat flux density ratio and the bottom heat transfer coefficient have little significant change with the increase of condensate mass flow rate (J_c).

5. Conclusion

1) Although condensation heat transfer coefficient at the bottom of the tube is at a low level (lower than a quarter of the vapor side), while with a significant

temperature difference, the heat flux density ratio is not small. So the heat transfer at the bottom should not be ignored.

- 2) The heat flux density ratio and the heat transfer coefficient ratio are obviously affected by the vapor quality. They will increase with the inlet velocity of the steam. But when the inlet velocity of the steam is higher than 47 m/s, the heat flux density ratio and the heat transfer coefficient ratio will not change with steam velocity. The heat flux density ratio and heat transfer coefficient at the bottom of tube have little relationship with the temperature difference of the steam and cooling water.
- 3) At a certain cross section, the wall temperature on the vapor side is almost the same but the temperature at the bottom is obviously low since the existing of condensate. At the end part of a long tube falling film evaporator, the temperature difference would reduce in a large extent. The tube length for a horizontal tube falling film evaporator is limited by the saturation temperature change.

- 4) The heat flux density ratio and heat transfer coefficient at the bottom of tube is mainly affected by the local vapor velocity. But they have little significant relationship with the condensate mass flow rate (J_c).

Symbols

B	— Heat transfer coefficient ratio
C	— Heat flux density ratio
F	— Heat transfer area of one tube-in-tube heat exchanger, m^2
J_c	— Condensate mass flow rate, g/s
L	— Total length of test section, m
Q_0	— Heat transfer of one tube-in-tube heat exchanger, J/s
Q_c	— The total heat transfer from the entrance of test section to the local test point, J/s
q_i	— Heat flux density, W/m^2
t_s	— Steam temperature, $^{\circ}C$
t_w	— Tube wall temperature, $^{\circ}C$
t_l	— Inlet temperature of cooling water, $^{\circ}C$
Δt	— Temperature difference of the steam and cooling water, $^{\circ}C$
Z	— Distance from the entrance of vapour, m
Z/L	— Inlet temperature of cooling water

Greek

α_{in}	— The average of condensation heat transfer coefficient, $W/(^{\circ}C \cdot m^2)$
α_{out}	— Heat transfer coefficients at the cooling water side, $W/(^{\circ}C \cdot m^2)$
δ	— Thickness of the condensate film, mm

Subscripts

s	— Steam side
c	— Condensate side

Acknowledgement

This research is supported by the Fundamental Research Funds for the Central Universities (DUT10ZD109 & DUT10RC(3)104), Shanghai Science and Technology innovation Scheme (No. 09DZ1200502), Liaoning Province Science and Technology Schemes (No. 2008220040, No. 20082173) and the foundation of Key Laboratory of Liaoning Province for Desalination.

References

- [1] M. Al-Shammiri and M. Safar, Multiple-effect distillation plants: state of the art, *Desalination*, 126 (1999) 45–59.
- [2] A. Ophir and F. Lokiec, Advanced MED process for most economical sea water desalination. *Desalination*, 182 (2005) 187–198.
- [3] M.A. Darwish, Desalination process: A technical comparison, Proc. IDA World Congress on Desalination and Water Sciences, Abu Dhabi, UAE, November 18–24, 1995, 1 (1995) 149–173.
- [4] H. Jaster and P.G. Kosky, Condensation heat transfer in a mixed flow regime. *Int. J. Heat Mass Transfer*, 19 (1976) 95–98.
- [5] W. Nusselt, Die Oberflächenkondensation des Wasser-dampfes. *Z. Ver. Dt. Ing.*, 60 (1916) 541–546.
- [6] A. Cavallini and G. Censi, Condensation inside and outside smooth and enhanced tubes — a review of recent research. *Int. J. Refrigeration*, 26 (2003) 373–392.
- [7] M.K. Dobson and J.C. Chato, Condensation in smooth horizontal tubes. *ASME J. Heat Transfer*, 120 (1998) 193–213.
- [8] B. Wang and X. Du, Experience study of condensation heat transfer in micro-tube. *J. Eng. Thermophysics*, 21 (2000) 324–328.
- [9] J.R. Thome and J.E. Hajal, Condensation in horizontal tubes. Part 2: New heat transfer model based on flow regimes. *Int. J. Heat Mass Transfer*, 46 (2003) 3365–3387.
- [10] N. Kattan, J.R. Thome and D. Favrat, Flow boiling in horizontal tubes. Part 3: Development of a new heat transfer model based on flow pattern, *J. Heat Transfer*, 120 (1998) 156–165.
- [11] B. Peng and Y. Li, Influence of Marangoni effect on film condensation inside a circular pipe. *Energy Eng.*, 3 (2007) 7–11.
- [12] S. Laohalertdecha and S. Wongwises, The effects of corrugation pitch on the condensation heat transfer coefficient and pressure drop of R-134a inside horizontal corrugated tube. *Int. J. Heat Mass Transfer*, 53 (2010) 2924–2931.
- [13] O. Baker, Design of pipe lines for simultaneous flow of oil and gas, *Oil Gas J.*, 26 (1954) 185–195.
- [14] J.M. Mandhane, G.A. Gregory and K. Aziz, A flow pattern map for gas-liquid flow in horizontal pipes, *Int. J. Multi-phase Flow*, 1 (1974) 537–553.
- [15] J.R. Thome, Update on advances in flow pattern based two-phase heat transfer models, *Int. J. Heat Mass Transfer*, 29 (2005) 341–349.
- [16] Y. Taitel and A.E. Dukler, A model for prediction flow regime transitions in horizontal and near horizontal gas-liquid flow, *AIChE J.*, 22 (1976) 47–55.
- [17] H.M. Soliman, On the annular-to-wavy flow pattern transition during condensation inside horizontal tubes, *Canad. J. Chem. Eng.*, 60 (1982) 475–481.
- [18] B. Mederic, P. Lavielle and M. Miscevic, Heat transfer analysis according to condensation flow structures in a mini-channel, *Experim. Thermal Fluid Sci.*, 30 (2006) 785–793.
- [19] A. Ophir, A. Gendel and G. Kronenberg, The LT-MED process for SW Cogen plants, *Desal. Water Reuse*, 4(1) (1994) 28–31.